Design and Analysis of Dual-Active-Bridge Converters in PVA Applications

P. Shamini[1] V.Srinivas[2]
[1]P.G. Student [2]Associate Professor
[1,2]Nigama Engineering College

Abstract— This paper proposes a DC-DC converter topology which converts the low voltage DC input of a PVA (Photo voltaic array) to a high gain output. The output of the converter is further inverted to interconnect various applications. The topology comprises of a dual active bridge (DAB) converter with a high frequency transformer. With increase in the switching frequency of the converter magnetizing losses are reduced as compared to other converters. The frequency of the DC to AC inverter at the output end is higher than the DAB converter, as an effect of increase in the efficiency of the topology. Several closed loop controllers (PI, feed forward, PIR) are used for the analysis of the converter. The total analysis in done in MATLAB simulink software and all the possible results are shown in the paper.

Key words: Dual-Active-Bridge Converters, PVA

I. INTRODUCTION

Replacement of fossil fuels with renewable energy resources is advancement in the electrical grid system. Generation of power through renewable energy power reduces injection the hazardous gases into the environment making a betterment to the green house effect. In these renewable energy power generation the wind and solar energy power generations are the most promising power generations of the category. Inducing of solar energy in to the grid is less complex and economical than the wind generation. However the wind system is considered to be a better option for its generation without power electronic devices which can produce pure sinusoidal waveform. The photo voltaic arrays produce very less power as compared to the wind system, where the voltage generated is also very less. The voltage of the PVA panels is in a range of 12v to 24V which is very much less when interconnected to grid. The output voltage of PV panels has to be increased through DC-DC converters.

In this paper we introduce a new topology with high switching frequency and high output gain value. With the high gain output voltage of the DC-DC converter it is flexible to connect the solar energy to the grid. The DAB DC-DC converter is shown in the figure below.

In the above figure we can observe that the input side is DC source which can be a PVA with a certain voltage level. The left converter is a high frequency inverter with a switching frequency of 100kHz. The DC output of the PVA is converted to high frequency AC by this inverter and fed to the isolation high frequency transformer with turns ratio 1:1. The right converter is a AC to DC converter which converts the high frequency AC output of the transformer to DC and fed to the DC load. To control the DAB circuit several control techniques are employed and which are given below.

- PI controller (PI)
- PI with feed forward control (PI-FF)
- PI with resonant control (PI-R)

A. PI controller (PI)

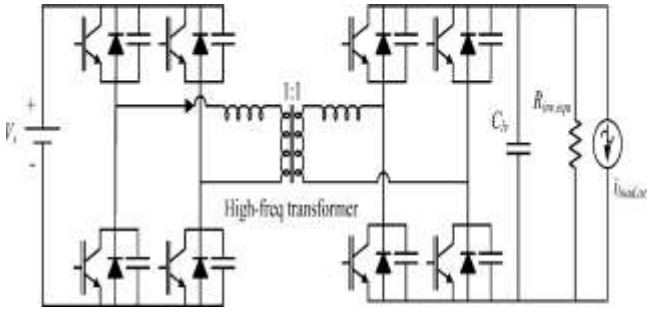

Fig. 1: DAB circuit for PVA application

The PI controller is a basic controller which controls the duty cycle of the switches with a delay angle between the primary side converter and the secondary side converter. The other two controllers are advancements to the PI controller to make the output stable in a lesser time. A simple PI control diagram is shown below designed in MATLAB simulink.

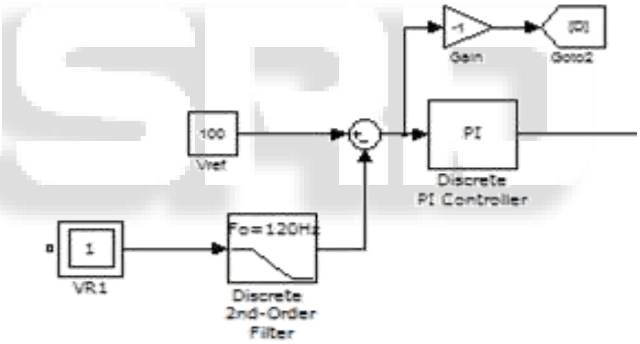

Fig. 2: PI control structure

The reference output voltage of the DAB converter is fed as Vref (100). The reference value of the voltage is compared to the output voltage at the load with a multi-meter. The error generated is the duty ratio which is fed to a PI controller which generates the delay time of the secondary side converter.

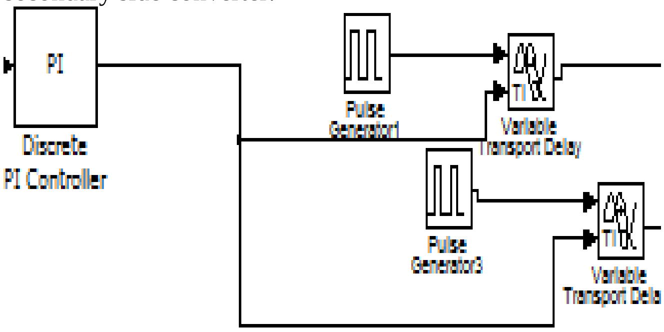

Fig. 3: Delay pulses generation

Further the delay time produced is fed to the transport delay block for change in the delay angle. The delay angle is fed to the pulses generators of the converter of the secondary side of the transformer. The power generated from the DAB converter is given as

$$P = \frac{v_s v_o}{2 f_s L_t} d(1-d)$$

Where, Vs = input voltage
Vo= output voltage
fs= switching frequency
Lt= transformer leakage inductance
d= phase shift ratio

B. PI with feed Forward Control (PI-FF)

In this control loop the PI controller is modified with a feed forward controller to improve the output of the converter with reducing the settling time. The feed forward control design is shown below.

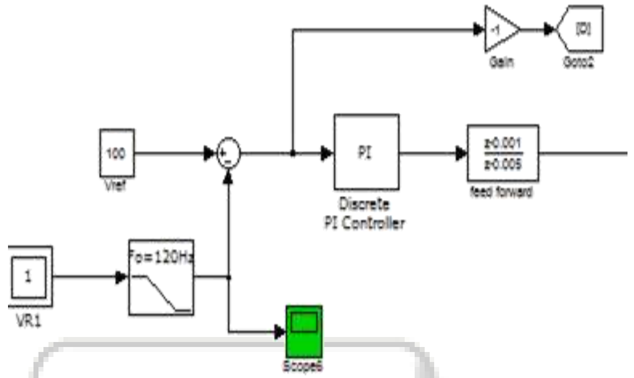

Fig. 4: PI – FF control design

A transfer function is used to increase the delay angle further taken as feed forward control which can increases the delay ratio for a instant of time making the output voltage settle faster. The power angle can be calculated as

$$\theta_p = 2\theta_v - \frac{\pi}{2}$$

Where, θv = output voltage phase angle

C. PI with resonant controller (PI-R)

In this controller a R controller is given to the PI controller with a transfer function given below.

$$G_{PR}(s) = K_r \frac{2s}{s^2 + \omega_2^2}$$

Where, Kr = resonant gain
w= 2*pi*f (f=120Hz)

The 'w' represents the second order harmonics of grid frequency. The simulink diagram is shown in the figure below

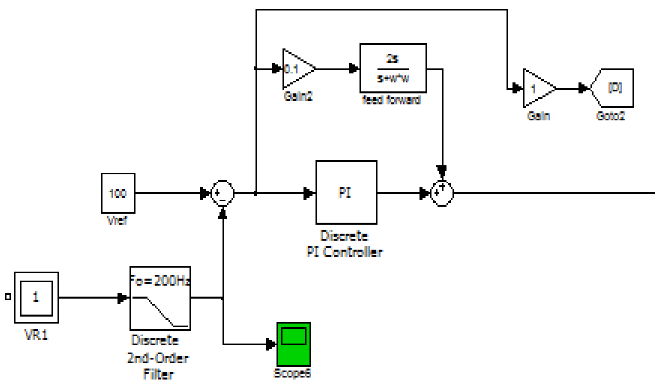

Fig. 5: PI-R controller

If an output voltage reference *v*ref is considered as reference and an inverter input current *i*inv is considered as disturbance, the output voltage *vo* in the frequency domain can be expressed as

$$v_o(s) = v_{ref}(s) \cdot G_1(s) + i_{inv} \cdot G_2(s)$$

Where,

$$G_1(s) = \frac{G_{PIR}(s) \cdot G_{vd}(s)}{1 + G_{PIR}(s) \cdot G_{vd}(s)}$$

$$G_2(s) = \frac{\frac{1}{sC_o}}{1 + G_{PIR}(s) \cdot G_{vd}(s)}$$

$$v_o = v_{ref} \cdot 1 + i_{inv} \cdot 0 = v_{ref}$$

$$\lim_{s \to 0} G_{PIR}(s) = +\infty$$

$$\lim_{s \to j\omega_2} G_{PIR}(s) = +\infty.$$

II. PVA SIMULINK MODEL

For efficient renewable power generation PVA is used to generate power from solar irradiation. As the load demand is increasing day by day the power generation also has to be increased, but due to the traditional way of power generation is causing global warming. Due to this the efficiency of the PVA has to be increased by adding silicon surface on the panel. And also employ MPPT techniques to track maximum power during any irradiation and atmospheric conditions. The design of PVA is done in MATLAB with Simulink block, with mathematical representation.

Voltage of PVA completely depends on solar irradiation (Sx) and ambient temperature (Tx). PVA (Photo voltaic array) is a combination of series and parallel solar cells arranged in an array to generated the required voltage and current. Each series combination of cells can be considered as photo voltaic module. Increase in series cells increases the voltage and increase in parallel cells increases the current capacity. Formulation for voltage of each cell is given below

$$V_c = \frac{AkT_c}{e} \ln\left(\frac{I_{ph} + I_0 - I_c}{I_0}\right) - R_s I_c$$

Where, k = Boltzmann constant (1.38 × 10-23 J/oK).
Ic = cell output current, Amp.
Iph = photocurrent
I0 = reverse saturation current of diode
Rs= series resistance of cell
Tc= reference cell operating temperature
Vc= cell voltage, V.

The Boltzmann constant and the reference temperature have to be in same units ie., either ^{0}C or ^{0}K. The mathematical modeling of the above equation can be constructed using simulink blocks is as below.

The above design is for a single cell voltage, in order to increase the voltage of the PVA the cell voltage has to be multiplied to a desired value considering each cell voltage as 0.4V. So, the number of series connected cells (Ns) can be calculated as

Ns = Vo/0.4

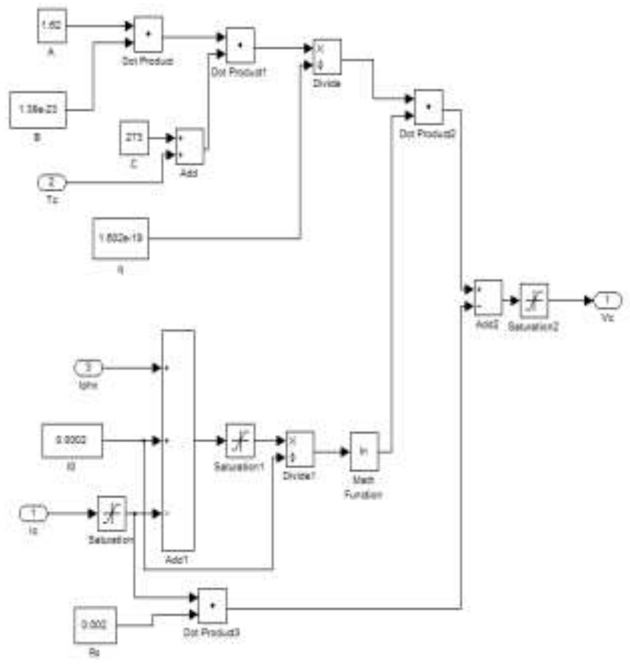

Fig. 6: Simulink model of Vc

To get each cell current, the total current output from the dependable source has to be divided by number of parallel connected cells (Np). Therefore, parallel connected cells are considered as

$$Np = Io/Icell$$

The representation in simulink is taken as

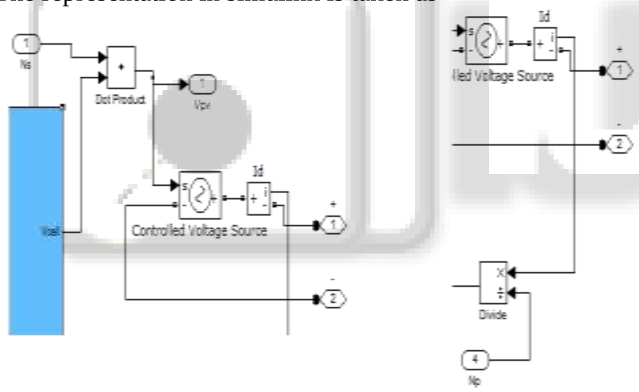

Fig. 7: Simulink modeling of Ns & Np

For the calculation of Vcx (cell voltage) and Iphx (Photocurrent) we need correction factors C_{TV} C_{TI} C_{SV} C_{SI}. The formulation is given as

$$V_{CX} = C_{TV} C_{SV} V_C$$

$$I_{phx} = C_{TI} C_{SI} I_{ph}$$

The correction factors are given as

$$C_{TV} = 1 + \beta_T (T_a - T_x)$$

$$C_{TI} = 1 + \frac{\gamma_T}{S_C} (T_x - T_a)$$

$$C_{SV} = 1 + \beta_T \alpha_S (S_x - S_C)$$

$$C_{SI} = 1 + \frac{1}{S_C} (S_x - S_C)$$

Where, $\beta_T = 0.004$ and $\gamma_T = 0.06$
Ta = reference temperature
Tx = ambient temperature
Sc = reference solar irradiation
Sx = ambient solar irradiation

The values of Tx and Sx changes depending upon the Sun rays which change continuously and unpredictably. The effect of change in solar irradiation varies the cell photocurrent and also the cell voltage (Vc). Let us consider the initial solar irradiation is I_{sx1} & the increase of the irradiation is I_{sx2} which in turn increases the temperature from T_{x1} to T_{x2}, photocurrent from I_{phx1} to I_{phx2}. The mathematical modeling of the correction factors in simulink is given below

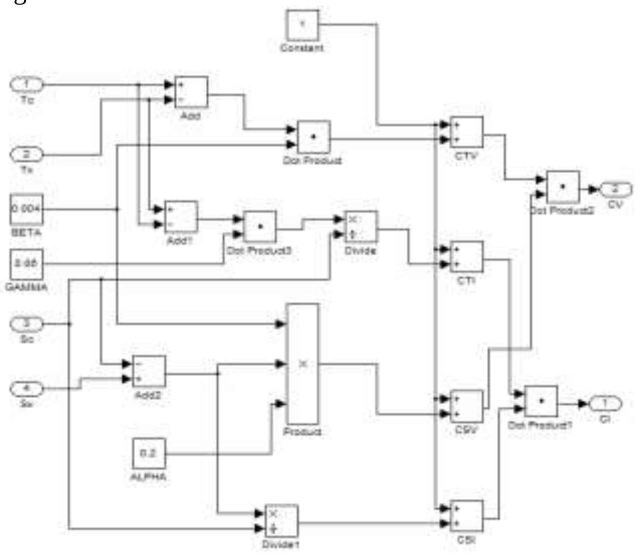

Fig. 8: CI & CV modelling

Depending upon the solar irradiation and temperature the values of CV & CI are calculated which is fed to Vc block to get the cell voltage value as shown below

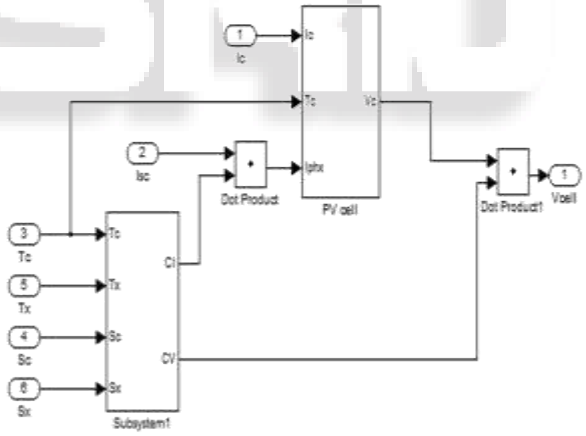

Fig. 9: Combined diagram of CV CI & Vc mathematical models

The total system diagram of the PVA with all the mathematical formulation are put into a subsystem to make it clear and understandable. The output of the Vc multiplied with the Ns constant block defining the total voltage of the combined cells of the PVA is fed to the voltage controlled voltage source block so as to generate the required voltage. A diode is connected in series at the positive terminal of the PVA to avoid reverse currents passing into the PVA. To reduce the ripples a capacitor can be added later after the diode in parallel as the capacitor doesn't allow sudden change of voltages dV/dt. The complete PVA module with internal block construction is shown in the fig. below

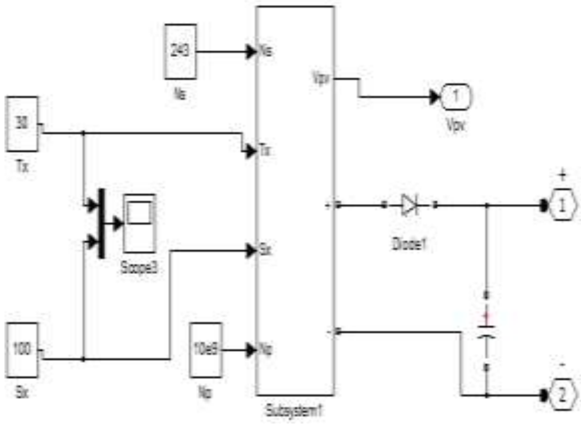

Fig. 10: Complete diagram of PVA

III. SIMULINK RESULTS

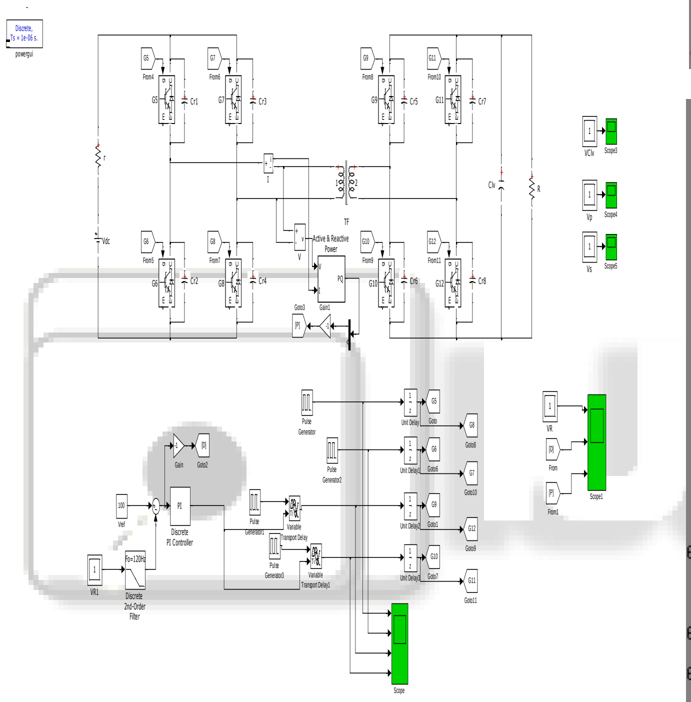

Fig. 11: complete simulink model of DAB

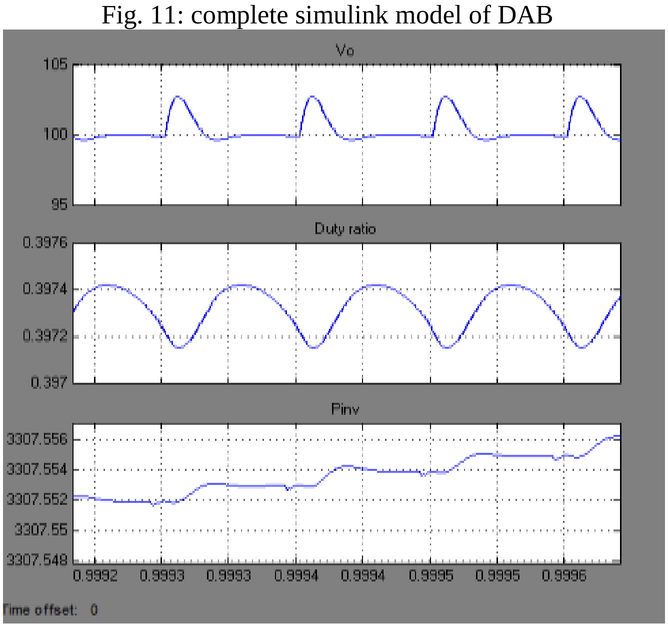

Fig. 12: output of only PI controller

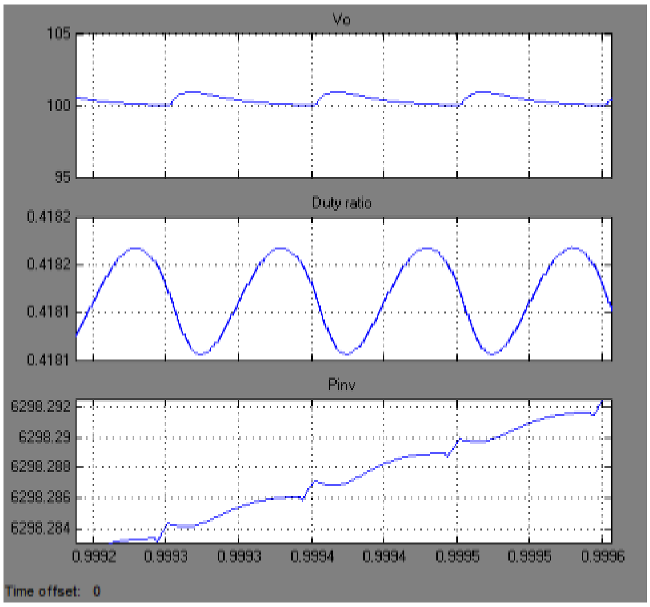

Fig. 13: output of PI controller with 4 times of C

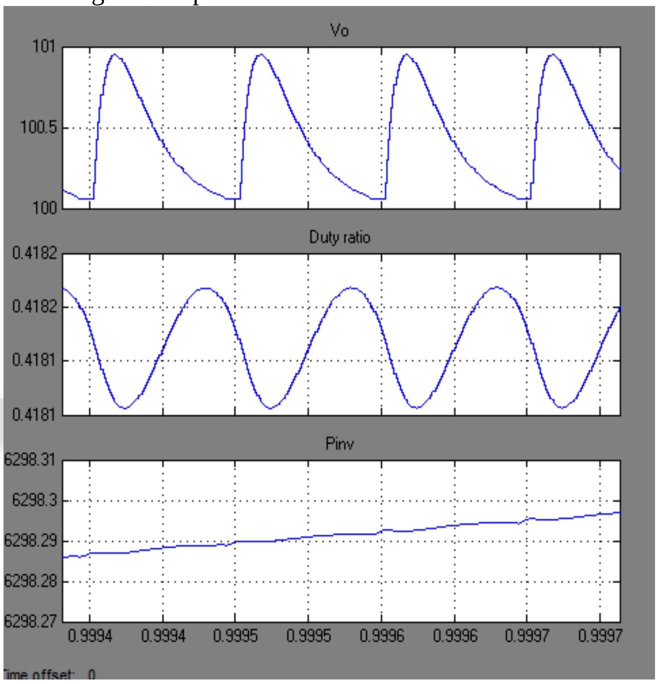

Fig. 14: outputs of PI controller with FF control

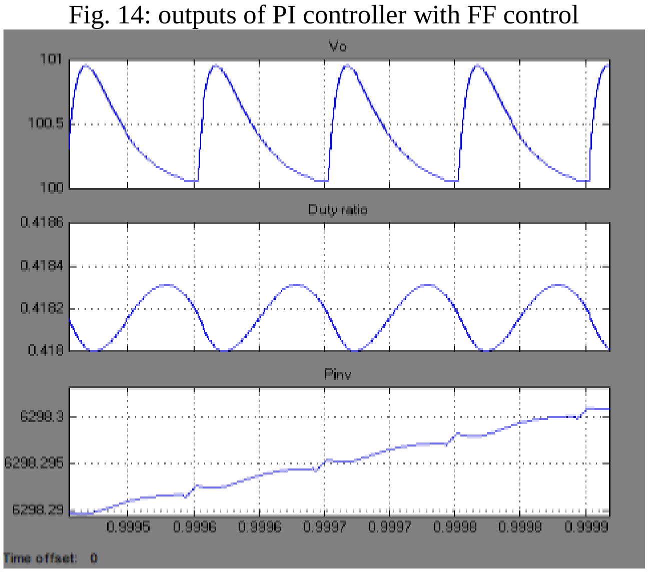

Fig. 15: outputs of PI-R controller

IV. CONCLUSION

With the above analysis and results with graphical representations the output voltage ripple can be controlled with the change of controller design. A comparison of all the controllers (PI, PI-FF, PI-R) is shown where the PI-R shows the best results as compared to the other two controllers. Ripple content in the output voltage are reduced to minimum with a value of 1% increasing the efficiency of the system.

REFERENCES

[1] A. Hasanzadeh, O. Onar, H. Mokhtari, and A. Khaligh, “A proportional-resonant controller-based wireless control strategy with a reduced number of sensors for parallel-operated UPSs,” IEEE Trans. Power Del., vol. 25, no. 1, pp. 468–478, Jan. 2010.
[2] A. Timbus, M. Liserre, R. Teodorescu, P. Rodriguez, and F. Blaabjerg, “Evaluation of current controllers for distributed power generation systems,” IEEE Trans. Power Electron., vol. 24, no. 3, pp. 654–664, Mar. 2009.
[3] Y. W. Li, F. Blaabjerg, D. Vilathgamuwa, and P. C. Loh, “Design and comparison of high performance stationary-frame controllers for DVR implementation,” IEEE Trans. Power Electron., vol. 22, no. 2, pp. 602–612, Mar. 2007.
[4] A. Yepes, F. Freijedo, O. Lopez, and J. Doval-Gandoy, “Analysis and design of resonant current controllers for voltage-source converters by means of Nyquist diagrams and sensitivity function,” IEEE Trans. Ind. Electron., vol. 58, no. 11, pp. 5231–5250, Nov. 2011.
[5] A. Roslan, K. Ahmed, S. Finney, and B. Williams, “Improved instantaneous average current-sharing control scheme for parallel-connected inverter considering line impedance impact in microgrid networks,” IEEE Trans. Power Electron., vol. 26, no. 3, pp. 702–716, Mar. 2011.
[6] P. Mattavelli, “Synchronous-frame harmonic control for high-performance ac power supplies,” IEEE Trans. Ind. Appl., vol. 37, no. 3, pp. 864–872, May/Jun. 2001.

